State Space Modeling of Variation Propagation in Multistation Machining Processes Considering Machining-Induced Variations

José V. Abellan-Nebot
Department of Industrial Engineering and Design,
Universitat Jaume I,
Castellón de la Plana E-12071, Spain
e-mail: abellan@uji.es

Jian Liu[1]
Department of Systems and
Industrial Engineering,
University of Arizona,
Tucson, AZ 85718
e-mail: jianliu@sie.arizona.edu

Fernando Romero Subirón
Department of Industrial Engineering and Design,
Universitat Jaume I,
Castellón de la Plana E-12071, Spain
e-mail: fromero@uji.es

Jianjun Shi
H. Milton Stewart School of Industrial and
Systems Engineering,
Georgia Institute of Technology,
Atlanta, GA 30332
e-mail: jianjun.shi@isye.gatech.edu

In spite of the success of the stream of variation (SoV) approach to modeling variation propagation in multistation machining processes (MMPs), the absence of machining-induced variations could be an important factor that limits its application in accurate variation prediction. Such machining-induced variations are caused by geometric-thermal effects, cutting-tool wear, etc. In this paper, a generic framework for machining-induced variation representation based on differential motion vectors is presented. Based on this representation framework, machining-induced variations can be explicitly incorporated in the SoV model. An experimentation is designed and implemented to estimate the model coefficients related to spindle thermal-induced variations and cutting-tool wear-induced variations. The proposed model is compared with the conventional SoV model resulting in an average improvement on quality prediction of 67%. This result verifies the advantage of the proposed extended SoV model. The application of the new model can significantly extend the capability of SoV-model-based methodologies in solving more complex quality improvement problems for MMPs, such as process diagnosis and process tolerance allocation, etc. [DOI: 10.1115/1.4005790]

Keywords: quality improvement, variation propagation modeling, differential motion vector, geometric-thermal variations, cutting-tool wear-induced variations, cutting force-induced variations

1 Introduction

Multistation Machining Processes (MMPs) are widely adopted in manufacturing industry for fabricating parts. In a MMP, a variety of machining operations are used to remove material from a rough-cast to achieve designated features and dimensional integrity. In order to ensure the modularity of the process, the machining operations are often divided into interconnected groups and performed on a series of work-stations. At each one of these stations, a workpiece is located and fixed by a fixture system according to a specific datum scheme to match part specifications.

Product quality improvement, in terms of reducing the geometric and/or dimensional variations of key product characteristics (KPCs), is essential, yet challenging for MMPs [1]. A quality product can be obtained when the entire MMP works under normal conditions and only inherent variations of the process are present. However, when assignable causes are present in a station of a MMP, excessive variations will be induced to the features, resulting in significant deviations from their nominal values [2]. If some of these deviating features are used in downstream stations as datum features, their deviations will be propagated and new random deviations will be generated, even though there is no more assignable causes present. As this scenario continues, the random deviations will keep propagating and accumulating to KPCs of final product. The evaluation of the KPC variations given process variations is of great concern in quality improving efforts, including product and process design optimization, in-process monitoring, and process variation sources identification. To successfully implement these activities, it is desirable to develop a mathematical modeling mechanism that explicitly describes the intrinsic variation induction and propagation in MMPs.

Variation propagation modeling has received intensive investigation in the recent decade. Various propagation models have been developed according to nominal product and process design information and off-line analysis of quality-process interactions and interstation correlations. For modeling the 2D variation propagation in multistation sheet metal assembly processes, Jin and Shi developed the state space modeling technique [3], which was further extended to 3D assembly processes [4,5]. For MMPs, Huang et al. [6] and Djurdjanovic and Ni [7] investigated the 3D variation propagation with an approximately linearized state space model. Zhou et al. [8] further generalized the deviation representation and proposed a generic linear state space model-based on differential motion vectors (DMVs). This generic model, named conventional SoV model, hereafter, considers three types of variation sources that are related to: datum surfaces that are used for locating the workpiece (datum-induced variations); fixture components that locate the workpiece on the machine-tool table (fixture-induced variations); and machining operations that generate the cutting-tool path (machining-induced variations). Recently, Abellan-Nebot et al. [9] demonstrated that overlooking the machining-induced variations in conventional SoV models may lead to inaccurate variation prediction. In an experiment of a three-station machining process, severe cutting-tool wear and significant spindle thermal expansion were intentionally added to the process. As a result, the model without considering such large machining-induced variations resulted in prediction errors at a level of 55.7%. Furthermore, the conventional SoV model presents the machining-induced errors as a cutting-tool path deviation, without providing a generic and explicit derivation procedure. Consequently, it cannot be readily applied to address key aspects of MMP design, such as evaluating the impacts of

[1]Corresponding author.

Contributed by the Manufacturing Engineering Division of ASME for publication in the Journal of Manufacturing Science and Engineering. Manuscript received March 28, 2010; final manuscript received November 24, 2011; published online March 30, 2012. Assoc. Editor: Steven J. Skerlos.

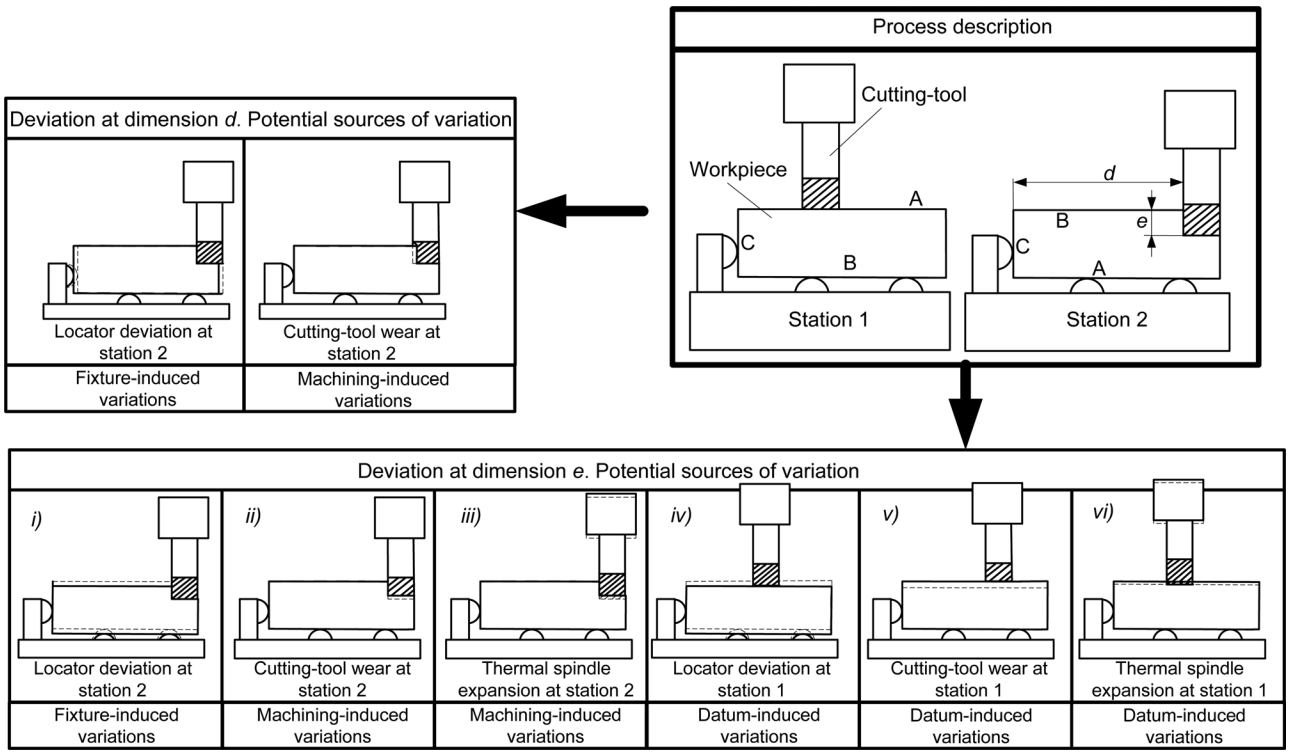

Fig. 1 Example of sources of variation in a MMP

cutting-tool wear or machine-tool thermal distortions on parts' dimensional variability.

In order to illustrate the current limitations of the conventional SoV model, we consider a two-station machining process shown in Fig. 1, where a face milling operation is conducted at the first station and the surface generated is used later as a datum feature at the second station for an end milling operation. Considering the dimensions d and e as two KPCs, it can be observed that besides the variations of fixture locators, (*i*) and (*iv*), the machining-induced variation sources also affect KPC dimensional quality. The induced variations include: cutting-tool wear-induced variations, as illustrated in (*ii*) and (*v*), and spindle thermal-induced variations, as illustrated in (*iii*) and (*vi*). Note that only the variations of datum features are considered as the datum-induced variations (Fig. 1). For this example, it is worthy to note that overlooking the explicit derivation of machining-induced variations may impair the prediction of the final product quality and the quality assurance decisions made based on it.

In order to overcome these limitations, it is desirable to develop a process-level methodology to include machining-induced variations from different sources in the state space model. According to the literature, four main sources of machining-induced variations can be distinguished [10,11], including: geometric-kinematic variations, thermal-induced variations, cutting force-induced variations, and cutting-tool wear-induced variations. At station-level, many research works have been conducted to model these machining sources of variation [12–19]. In general, these models require the experimental procedures since the model derivation depends on specific machining operation conditions (cutting parameters, coolant types, machine-tool conditions, etc.). For instance, the evaluation of geometric-kinematic variations depends on positioning errors, straightness errors and angular errors of machine-tool axes and squareness errors between axes. These types of errors can be measured with laser interferometers [14] or 3D probe-balls [15]. The evaluation of thermal-induced variations also requires an experimental procedure with the use of several temperature sensors throughout the machine-tool structure [12]. Other machining-induced variations, such as those related to cutting forces and tooling wear, require parameters of cutting-tool geometry and frequency response properties, which can be estimated from the experimental data [13,16–19]. Figure 2 summarizes the required parameters to model machining-induced variations and some research works conducted for station-level modeling.

In this paper, a generic framework of the state space formulation based on DMVs is proposed to explicitly model the induction and propagation of machining-induced variations. In addition, an experimentation is designed and implemented to estimate the model coefficients corresponding to cutting-tool wear-induced and spindle thermal-induced variations. The proposed model will provide quality improvement practitioners with a more comprehensive tool for more accurate and precise evaluation, and thus, more effective monitoring and diagnosis of MMPs. The remainder of this paper is organized as follows. Section 2 introduces the formulation of the state space model and the deviation representation mechanism adopted in this paper. Section 3 presents the proposed generic framework for machining-induced variation modeling, together with the detail experimental procedure to model spindle thermal-induced variations and cutting-tool wear-induced variations through flank wear and spindle temperature measurements. A case study is conducted and summarized in Sec. 4 for model validation. Concluding remarks and potential model applications are discussed in Sec. 5.

2 Random Deviation Representation

In the conventional SoV model, datum-, machining-, and fixture-induced variations are considered. These types of variations are induced by and transmitted among seven key elements of machining stations: (i) machine-tool structure, (ii) axes of the machine-tool, (iii) machine-tool spindle, (iv) cutting-tool, (v) fixture locators, (vi) workpiece datum features, and (vii) manufactured features. Describing the SoV is equivalent to representing the transmission and transformation of those types of variations among these elements.

2.1 Coordinate System Definition. In order to represent the dimensional variations of the seven elements involved in the SoV model, different coordinate systems (CSs) are defined.

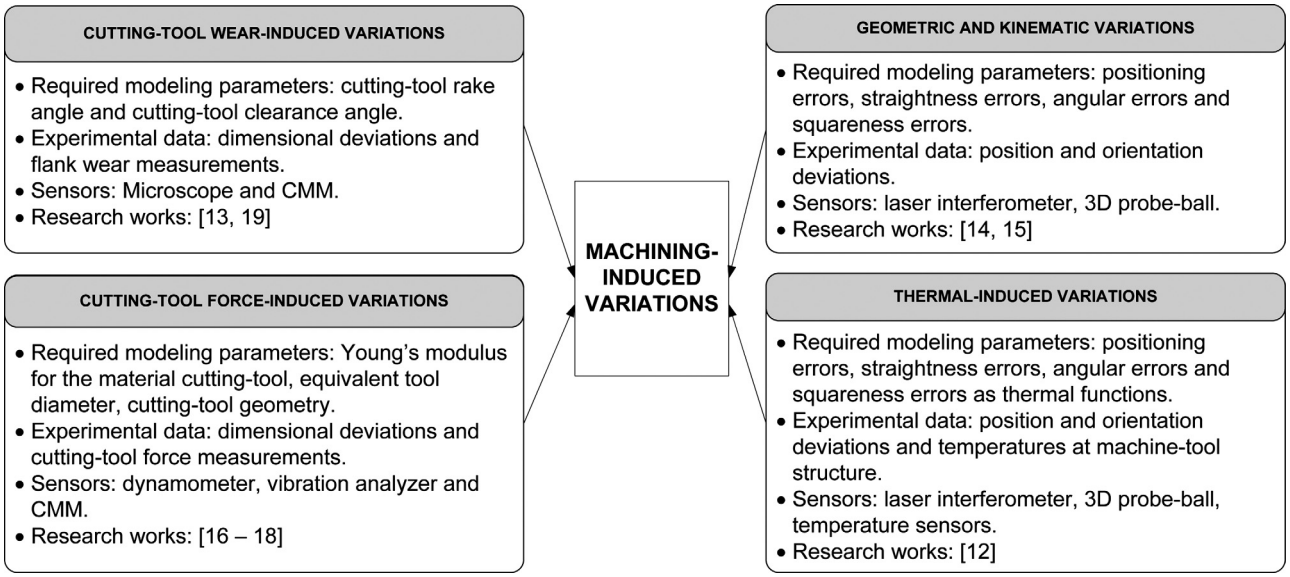

Fig. 2 Required modeling parameters for estimating machining-induced variations

2.1.1 Design Coordinate System (DCS). The nominal DCS, denoted as $^{\circ}D$, define the reference for the workpiece features during design. The definition of $^{\circ}D$ usually depends on the nominal geometry of the part. It is usually defined at an accessible corner. As this CS is only used in design, this CS will not deviate.

2.1.2 Reference Coordinate System (RCS). The nominal and the true RCS, denoted as $^{\circ}R_k$ and R_k, respectively, define the reference for all the workpiece features (Fig. 3(*d*)) at station k. To simplify the model derivation, the R_k is defined the same as the local CS of the primary datum feature at station k. In a 3-2-1 fixture layout, the primary datum is the main workpiece surface used to locate the part at the machine-tool table [20].

2.1.3 Fixture Coordinate System (FCS). The nominal and the true FCS at station k, denoted as $^{\circ}F_k$ and F_k, respectively, define the physical position and orientation of the fixture device according to the fixture layout. Figure 3(*d*) shows the FCS for a fixture layout based on the 3-2-1 principle.

2.1.4 Local Coordinate System (LCS^j). The nominal and the true LCS^j at station k, denoted as $^{\circ}L_k^j$ and L_k^j, define the physical position and orientation of the jth nominal and actual surface of the part, respectively (Fig. 3(*c*)). For planar surfaces the Z-axis of $^{\circ}L_k^j$ is commonly defined normal to the surface.

2.1.5 Machine-Tool Coordinate System (MCS). The MCS at station k, denoted as $^{\circ}M_k$, define the physical position and orientation of the reference CS for machine-tool movements. The origin of the $^{\circ}M_k$ is located at the locating origin of the nominal machine-tool table, with its Z-axis normal to the table and pointing upward, its X-axis parallel to the long axis of the table and pointing to its positive direction, and its Y-axis defined according to the right hand rule (RHR), as shown in Fig. 3(*a*). In this paper, it is assumed that $^{\circ}M_k$ serves as the reference at station k and thus will not deviate.

2.1.6 Axis Coordinate System (ACS^i). The nominal and the true ACS of the ith axis used at station k, denoted as $^{\circ}A_k^i$ and A_k^i, respectively, define the physical position and orientation of the ith machine-tool axis. The origin of the $^{\circ}A_k^i$ is located at the geometrical center of the joint of the ith axis. For prismatic joints, the axes of the $^{\circ}A_k^i$ have the same orientation as that of the $^{\circ}M_k$. For revolute joints, the Z-axis of the $^{\circ}A_k^i$ coincides with the rotation axis with the same positive direction. Its X- and Y-axes are parallel to the axes of $^{\circ}M_k$ and their orientations are defined according to the RHR. For a 5-axis machine-tool, the ACSs of machine-tool axes are shown in Fig. 3(*a*). The A_k^i is similarly defined for an actual axis.

2.1.7 Spindle Coordinate System (SCS). The nominal and the true SCS at station k, denoted as $^{\circ}S_k$ and S_k, respectively, define the physical position and orientation of the spindle during machining. The origin of the $^{\circ}S_k$ is located at the geometrical center of the spindle and the orientations of axes are identical to that of the Z-axis of MCS, as shown in Fig. 3(*b*). The S_k is defined similarly for the actual spindle.

2.1.8 Cutting-Tool Coordinate System (CCS). The nominal and the true CCS at station k, denoted as $^{\circ}C_k$ and C_k, respectively, define the physical position and orientation of the cutter tip center during machining. The origin of the $^{\circ}C_k$ is located at the cutter tip center and the orientations of its axes are identical to that of the S_k, as shown in Fig. 3(*c*). The C_k is defined similarly for the actual cutting-tool.

2.1.9 Cutting-Tool Tip Coordinate System (TPCS). The nominal and the true TPCS at station k, denoted as $^{\circ}P_k$ and P_k, respectively, defines the physical position and orientation of the cutting-tool tip. The origin of the $^{\circ}P_k$ is located at the center of the cutting edge that is used to generate a feature j, and the orientations of its axes are parallel to that of $^{\circ}L_k^j$. Please note that, when machining a feature j at station k, the cutting-tool tip removes material generating the machined feature which is defined by the L_k^j. Thus, the position and orientation of the P_k define the position and orientation of L_k^j, as shown in Fig. 3(*c*).

The CSs defined above establish a generic framework for representing the variation induction and transmission along a chain from the cutting-tool tip to the jth manufacturing feature, i.e., from P_k to $^{\circ}D$. The whole chain is composed of two subchains. The first subchain, defined from $^{\circ}M_k$ to P_k, represents how machining-induced variations deviate the cutting-tool tip w.r.t. the machine-tool CS (MCS). The most common machining-induced variations are due to geometric and kinematic errors of machine-tool axes, thermal distortions, cutting-tool deflections, and cutting-tool wear, which introduce random deviations to A_k^i, S_k, C_k, and P_k. The second subchain, defined from $^{\circ}M_k$ to $^{\circ}D$, represents how fixture- and datum-induced variations deviate the workpiece location w.r.t. the MCS.

2.2 Variation Representation. The position and the orientation of a CS can be defined by a vector consisting of a positioning vector and an orientation vector w.r.t. another CS. For instance,

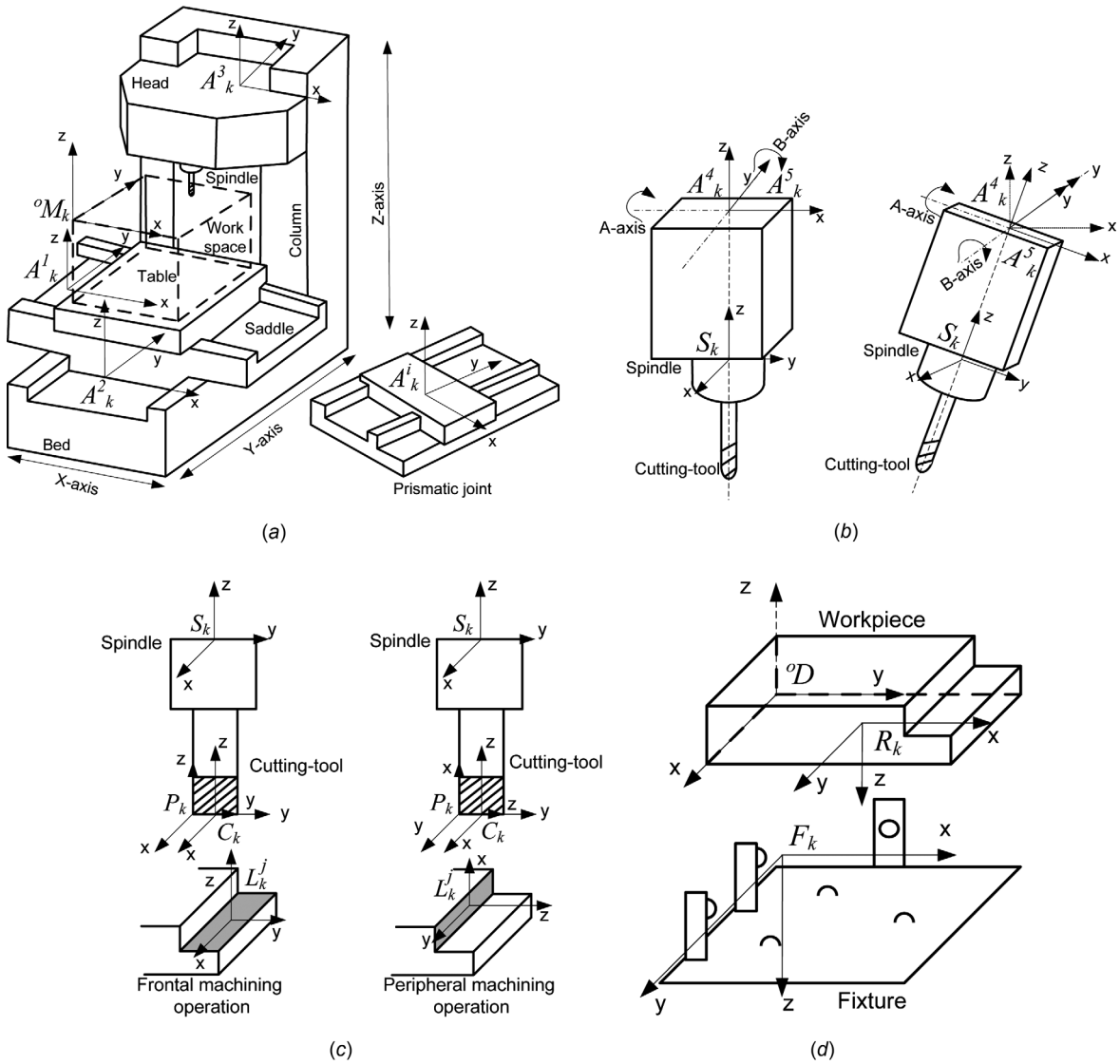

Fig. 3 Example of the CSs involved in a 5-axis CNC machine-tool

CS_1 can be defined, w.r.t. CS_2, as $\mathbf{r}_1^2 = \left[(\mathbf{t}_1^2)^T (\boldsymbol{\omega}_1^2)^T\right]^T$, where $\mathbf{t}_1^2 = \begin{bmatrix} x_1^2 & y_1^2 & z_1^2 \end{bmatrix}^T$ and $\boldsymbol{\omega}_1^2 = \begin{bmatrix} \alpha_1^2 & \beta_1^2 & \gamma_1^2 \end{bmatrix}^T$. This indicates that the projections of CS_1 on the three coordinates of CS_2, X_2, Y_2, and Z_2, are x_1^2, y_1^2, and z_1^2, respectively. The orientation of the axes X_1, Y_1, and Z_1 can be obtained by sequentially rotating CS_2 around Z_2, Y_2' (after the first rotation) and Z_2'' (after the second rotation) with Euler angles of α_1^2, β_1^2, and γ_1^2, respectively.

Based on the CS definitions and the vectorial CS representations, the random deviation of an element involved in the machining process, e.g., a machine-tool spindle, can be represented by a DMV [21] of its own CS w.r.t. another CS. For instance, CS_1 is the SCS of a spindle and CS_2 is the MCS of a machine-tool. The nominal position and orientation of the spindle of a machine-tool are defined by $\mathbf{r}_1^2$. The random deviation of the spindle w.r.t. the machine-tool can be defined by the DMV $\mathbf{x}_1^2$, where $\mathbf{x}_1^2 = \left[(\mathbf{d}_1^2)^T (\mathbf{s}_1^2)^T\right]^T$, $\mathbf{d}_1^2$ contains three small position deviations, i.e., $\mathbf{d}_1^2 = \begin{bmatrix} \Delta x_1^2 & \Delta y_1^2 & \Delta z_1^2 \end{bmatrix}^T$, and $\mathbf{s}_1^2$ contains three small orientation deviations, i.e., $\mathbf{s}_1^2 = \begin{bmatrix} \Delta\alpha_1^2 & \Delta\beta_1^2 & \Delta\gamma_1^2 \end{bmatrix}^T$.

The DMV representation of random deviations among CSs creates the basis of the variation propagation model. The induction, transmission, and accumulation of deviations are modeled along the chain of CSs as a series of transformations of DMVs among different CSs. These transformations are linearized by assuming that the magnitudes of DMV elements are small and are mathematically represented by the following lemma [8]:

Lemma 1. *Consider the CSs R, 1 and 2 as shown in Fig. 4, with CSs 1 and 2 deviating from their nominal positions and orientations. Noting the deviation of CS 1 w.r.t. reference CS R as* $\mathbf{x}_1^R$ *and the deviation of CS 2 w.r.t. the CS 1 as* $\mathbf{x}_2^1$*, then, the deviation of CS 2 w.r.t. CS R can be formulated as*

$$\boldsymbol{x}_2^R = \begin{pmatrix} \left(\boldsymbol{R}_{\circ 2}^{\circ 1}\right)^T & -\left(\boldsymbol{R}_{\circ 2}^{\circ 1}\right)^T \cdot \left(\hat{\boldsymbol{t}}_{\circ 2}^{\circ 1}\right) & \boldsymbol{I}_{3\times 3} & \boldsymbol{0} \\ \boldsymbol{0} & \left(\boldsymbol{R}_{\circ 2}^{\circ 1}\right)^T & \boldsymbol{0} & \boldsymbol{I}_{3\times 3} \end{pmatrix} \cdot \begin{pmatrix} \boldsymbol{x}_1^R \\ \boldsymbol{x}_2^1 \end{pmatrix} = \boldsymbol{T}_2^1 \cdot \boldsymbol{x}_1^R + \boldsymbol{x}_2^1 \tag{1}$$

where $\boldsymbol{R}_{\circ 2}^{\circ 1}$ *is the rotation matrix of* CS °2 *w.r.t.* CS °1, $\boldsymbol{I}_{3\times 3}$ *is a* 3×3 *identity matrix and* $\hat{\boldsymbol{t}}_{\circ 2}^{\circ 1}$ *is the skew matrix of vector* $\boldsymbol{t}_{\circ 2}^{\circ 1}$.

The proof of this lemma can be found in [8], and it is shown in the Appendix. This lemma is intensively used in this paper to derive the deviation transmission among different CSs.

3 Extension of the State Space Model

Based on the vectorial deviation representation with DMVs, variation propagation in MMPs can be described with a state

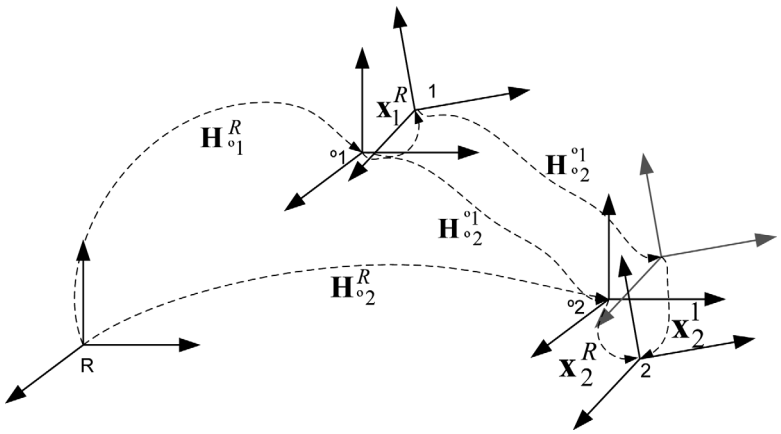

Fig. 4 DMV from CS 2 to CS 1 if both CSs deviate from nominal values

space model [8]. The deviations that have been generated on a workpiece after station k are represented as a state vector, $\mathbf{x}_k$, which is a stack of the DMVs of all the manufacturing features. Assuming that at station k there are M features on a workpiece, and the deviation of the cth $(c=1,2,\ldots,M)$ feature w.r.t. the RCS is represented as a 6×1 DMV, $\mathbf{x}^R_{k,c}$, the state vector is described as $\mathbf{x}_k=[(\mathbf{x}^R_{k,1})^T \quad (\mathbf{x}^R_{k,2})^T \quad \cdots \quad (\mathbf{x}^R_{k,M})^T]^T$, where $\mathbf{x}_k \in \Re^{6M\times 1}$. Denoting the datum deviation introduced from station $k-1$ as $\mathbf{x}_{k-1}$, the fixture- and machining-induced deviations at station k as $\mathbf{u}_k$, and the deviations of the KPCs measured at station k as $\mathbf{y}_k$, the variation propagation model for an N-station MMP is formulated as

$$\mathbf{x}_k = \mathbf{A}_{k-1}\cdot\mathbf{x}_{k-1} + \mathbf{B}_k\cdot\mathbf{u}_k + \mathbf{w}_k \tag{2}$$

$$\mathbf{y}_k = \mathbf{C}_k\cdot\mathbf{x}_k + \mathbf{v}_k \tag{3}$$

where $k=1,2,\ldots,N$. In the station transition equation (2), $\mathbf{A}_{k-1}\cdot\mathbf{x}_{k-1}$ represents the deviations transmitted by datum features generated at upstream stations; $\mathbf{B}_k\cdot\mathbf{u}_k$ represents the deviations introduced within station k, including those from fixture locators and by machining operations. In the observation equation (3), $\mathbf{C}_k\cdot\mathbf{x}_k$ represents the deviations of KPCs, measured from the manufactured features. The terms $\mathbf{w}_k$ and $\mathbf{v}_k$ define the unmodeled system errors (e.g., linealization errors) and the measurement noise, respectively.

In the conventional SoV model formulation [8], only the fixture-induced variations and an overall cutting-tool path variations are considered in $\mathbf{u}_k$. In that model, $\mathbf{u}_k$ is defined as $\mathbf{u}_k=\left[(\mathbf{u}^k_f)^T \quad (\mathbf{u}^k_m)^T\right]^T=\left[\Delta l^k_1\ \Delta l^k_2\ \Delta l^k_3\ \Delta l^k_4\ \Delta l^k_5\ \Delta l^k_6\ (\mathbf{u}^k_m)^T\right]^T$, where $\mathbf{u}^k_f$ is the deviation of the fixture components (Δl^k_i is the deviation of the ith fixture locator from their nominal position at station k), and $\mathbf{u}^k_m$ is the overall cutting-tool path deviation that models the overall deviation of the CS of the jth machined feature, L^j_k, from the nominal fixture CS, $^\circ F_k$, i.e., $\mathbf{x}^{^\circ F_k}_{L^j_k}$. However, this formulation does not explicitly model any specific machining-induced variation, such as those due to geometric-thermal effects, cutting-tool wear or cutting-tool deflections. In Sec. 3.1 , an extension of the conventional state space model to incorporate machining-induced variations will be proposed.

3.1 Framework for Incorporating Machining-Induced Variations. In this paper, the manufacturing features are obtained from material removal by the cutting-tool edge. Thus, the overall cutting-tool path deviation of a manufactured feature, $\mathbf{x}^{^\circ F_k}_{L^j_k}$, is equivalent to the deviation of the cutting-tool edge, represented by the TPCS P_k, from the nominal fixture CS, $\mathbf{x}^{^\circ F_k}_{P_k}$, i.e., $\mathbf{x}^{^\circ F_k}_{L^j_k}\equiv\mathbf{x}^{^\circ F_k}_{P_k}$. In this context, the incorporation of machining-induced variations can be built upon investigating the variations along the chain of CSs from the TPCS, P_k, to the nominal FCS, $^\circ F_k$, at station k.

Figure 5 shows the relationship between the different CSs at station k where a generic n-axis machine-tool is used. All the elements involved in that station are defined by their corresponding CSs, composing a chain of CSs. Every nominal CS is defined w.r.t. its previous nominal CS in the chain, through a homogeneous transformation matrix (HTM). Due to fixture- and machining-induced variations, the CSs are deviated from their nominals by a DMV. Thus, at station k, the final cutting-tool path deviation defined by the DMV $\mathbf{x}^{^\circ F_k}_{P_k}$ will be affected by the DMVs of all the CSs in the chain. Applying Lemma 1 repeatedly, one can express the total cutting-tool path deviation $\mathbf{x}^{^\circ F_k}_{P_k}$ as a function of all CSs' deviations according to the following expression:

$$\mathbf{x}^{^\circ F_k}_{P_k}=\mathbf{x}^{^\circ M_k}_{P_k}=\mathbf{T}^{C_k}_{P_k}\cdot\left(\mathbf{T}^{S_k}_{C_k}\cdot\left(\mathbf{T}^{A^n_k}_{S_k}\cdot\mathbf{x}^{^\circ M_k}_{A^n_k}+\mathbf{x}^{A^n_k}_{S_k}\right)+\mathbf{x}^{S_k}_{C_k}\right)+\mathbf{x}^{C_k}_{P_k} \tag{4}$$

where the DMV terms are linked with the following machining-induced variations:

(i) The geometric, kinematic, and thermal variations of machine-tool axes are represented by a DMV, $\mathbf{x}^{^\circ M_k}_{A^n_k}$, of the true ACS, A^n_k, w.r.t. the nominal MCS, $^\circ M_k$. It is modeled as

$$\mathbf{x}^{^\circ M_k}_{A^n_k}=\mathbf{B}^{m_1}_k\cdot[\Delta T^k_1 \quad \ldots \quad \Delta T^k_m \quad (\Delta\mathbf{r}^k)^T]^T \tag{5}$$

The deviation at the nth axis of a machine-tool due to the thermal expansion can be related to the temperature deviations from nominal values (cold conditions) at m different locations on the machine-tool structure, i.e., $\Delta T^k_1,\ldots,\Delta T^k_m$. On the other hand, the deviation at the nth axis of a machine-tool due to geometric and kinematic effects is related to the deviation of the placement of the workpiece on the machine-tool table. If the workpiece was always placed on the machine-tool exactly at the same position, the geometric and kinematic deviations would be negligible since the deviation would be a constant value, which can be easily compensated. Thus, the geometric and kinematic deviation of the nth machine-tool axis is a function of the deviation of the workpiece placement from nominal values, denoted as $\Delta\mathbf{r}^k$. Please note that the nominal values of temperatures and placement of the workpiece should be defined for the linealization of the geometric-thermal variations. As this paper is focused on modeling and analyzing random deviations in MMPs, we discard the systematic deviations due to linealization since they can be compensated by calibration. The derivation of $\mathbf{B}^{m_1}_k$ is introduced in Sec. 3.2.

(ii) The spindle-thermal variations are represented by a DMV, $\mathbf{x}^{A^n_k}_{S_k}$, of the true SCS, S_k, w.r.t. the true ACS, A^n_k. It is modeled as

$$\mathbf{x}^{A^n_k}_{S_k}=\mathbf{B}^{m_2}_k\cdot[\Delta T^k_s] \tag{6}$$

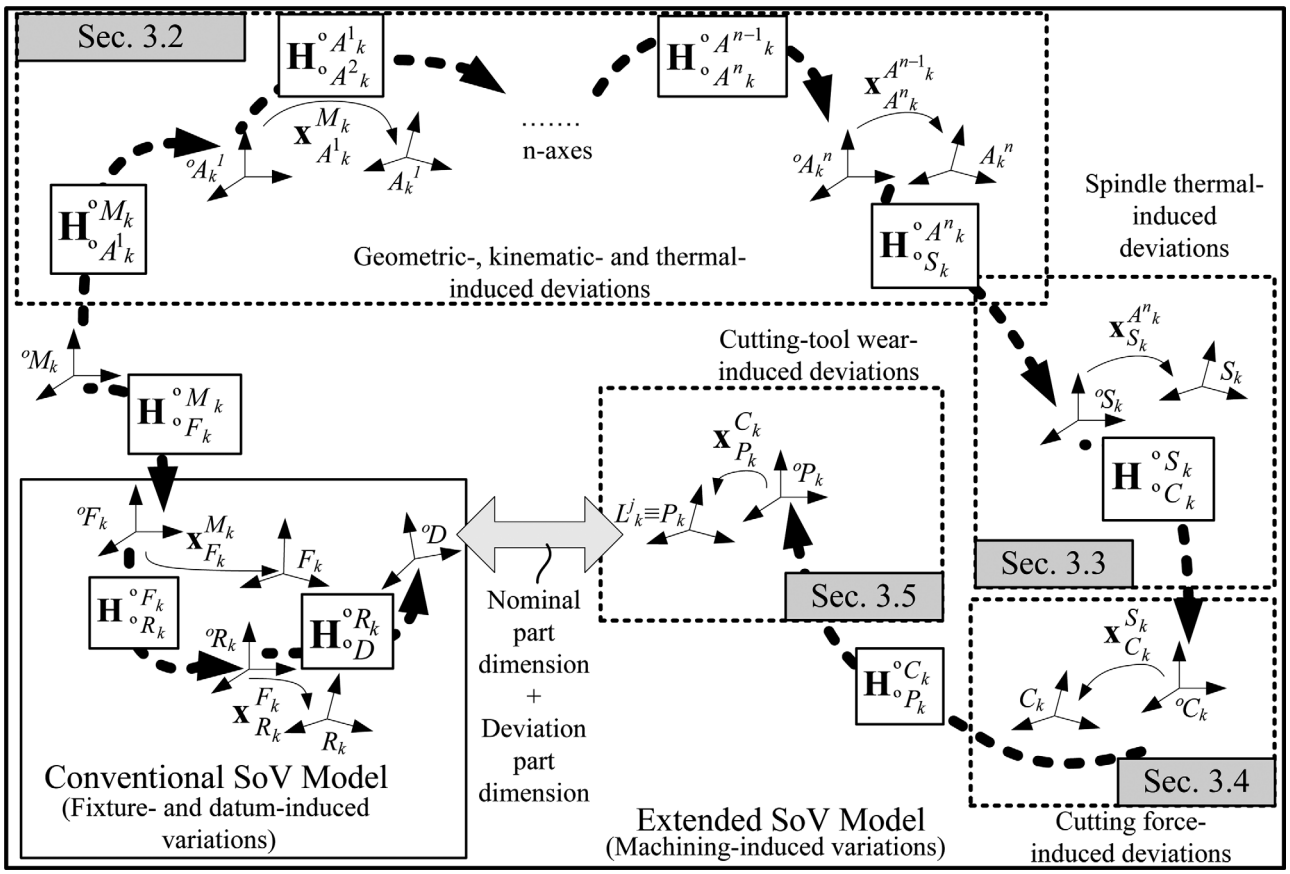

Fig. 5 Relationships between the different CSs in a *n*-axis machine-tool

The deviation of the spindle due to its thermal expansion is a function of the spindle temperature variation ΔT_s^k. The derivation of $\mathbf{B}_k^{m_2}$ is introduced in Sec. 3.3.

(iii) The cutting force-induced variations are represented by a DMV, $\mathbf{x}_{C_k}^{S_k}$, of the true CCS, C_k, w.r.t. the true SCS, S_k. It is modeled as

$$\mathbf{x}_{C_k}^{S_k} = \mathbf{B}_k^{m_3} \cdot [\Delta F_x^k \quad \Delta F_y^k]^T \tag{7}$$

The deviation of the cutting-tool due to deflections is a function of the variations of the cutting forces ΔF_x^k and ΔF_y^k. The derivation of $\mathbf{B}_k^{m_3}$ is introduced in Sec. 3.4.

(iv) The cutting-tool wear-induced variations are represented by a DMV, $\mathbf{x}_{P_k}^{C_k}$, of the true TPCS, P_k, w.r.t. the true CCS, C_k.

$$\mathbf{x}_{P_k}^{C_k} = \mathbf{B}_k^{m_4} \cdot [V_{B_{ij}}^k] \tag{8}$$

The deviation of the cutting-tool tip is a function of the cutting-tool wear at the cutting edge, $V_{B_{ij}}^k$, where i and j indicate the ith cutting edge of the jth cutting-tool. The derivation of $\mathbf{B}_k^{m_4}$ is introduced in Sec. 3.5.

Based on the elaboration of the four DMV terms, Eq. (4) can be rewritten as

$$\mathbf{x}_{P_k}^{\circ F_k} = [\mathbf{T}_{P_k}^{C_k} \cdot \mathbf{T}_{C_k}^{S_k} \cdot \mathbf{T}_{S_k}^{A_k^n} \cdot \mathbf{B}_k^{m_1} \ \vdots \ \mathbf{T}_{P_k}^{C_k} \cdot \mathbf{T}_{C_k}^{S_k} \cdot \mathbf{B}_k^{m_2} \ \vdots \ \mathbf{T}_{P_k}^{C_k} \cdot \mathbf{B}_k^{m_3} \ \vdots \ \mathbf{B}_k^{m_4}] \cdot [\Delta T_1^k \ \ldots \ \Delta T_m^k \ \Delta x^k \ \Delta y^k \ \Delta z^k \ \Delta\alpha^k \ \Delta\beta^k \ \vdots \ \Delta T_s^k \ \vdots \ \Delta F_x^k \ \Delta F_y^k \ \vdots \ V_{B_{ij}}^k]^T \tag{9}$$

This formulation can be incorporated into the model (2), where $\mathbf{B}_k \cdot \mathbf{u}_k$ is defined as

$$\mathbf{B}_k \cdot \mathbf{u}_k = [\mathbf{B}_f^k \ \vdots \ \mathbf{B}_m^k] \cdot [(\mathbf{u}_f^k)^T \ \vdots \ (\mathbf{u}_m^k)^T]^T \tag{10}$$

and $\mathbf{B}_f^k$ models the impacts of the deviations of fixture locators, $\mathbf{u}_f^k$; $\mathbf{B}_m^k$ is a selector matrix $\mathbb{A}_5^k$, (see Ref. [8]), to specify the feature machined at station k; and $\mathbf{u}_m^k$ is the DMV $\mathbf{x}_{L_k^j}^{\circ F_k}$, which is equivalent to the DMV $\mathbf{x}_{P_k}^{\circ F_k}$ in this paper. Therefore, the conventional SoV model can be extended by plugging Eq. (9) into Eq. (10). The term $\mathbf{B}_k \cdot \mathbf{u}_k$ in the extended SoV model is

$$\mathbf{B}_k \cdot \mathbf{u}_k = [\mathbf{B}_f^k \ \vdots \ \mathbb{A}_5^k \cdot \mathbf{T}_{P_k}^{C_k} \cdot \mathbf{T}_{C_k}^{S_k} \cdot \mathbf{T}_{S_k}^{A_k^n} \cdot \mathbf{B}_k^{m_1} \ \vdots \ \mathbb{A}_5^k \cdot \mathbf{T}_{P_k}^{C_k} \cdot \mathbf{T}_{C_k}^{S_k} \cdot \mathbf{B}_k^{m_2} \ \vdots \ \mathbb{A}_5^k \cdot \mathbf{T}_{P_k}^{C_k} \cdot \mathbf{B}_k^{m_3} \ \vdots \ \mathbb{A}_5^k \cdot \mathbf{B}_k^{m_4}] \cdot [(\mathbf{u}_f^k)^T \ \vdots \ \Delta T_1^k \ \ldots \ \Delta T_m^k \ \Delta x^k \ \Delta y^k \ \Delta z^k \ \Delta\alpha^k \ \Delta\beta^k \ \vdots \ \Delta T_s^k \ \vdots \ \Delta F_x^k \ \Delta F_y^k \ \vdots \ V_{B_{ij}}^k]^T \tag{11}$$

A summary of the procedure to obtain the state space model incorporating machining-induced variations is shown in Fig. 6. As it can be noted, part of the procedure is based on the conventional procedure to derive the state space model, as shown in Ref. [8]. The rest of the procedure is the proposed extension model where each type of machining-induced variation is modeled and added into the state space model.

Sections 3.2–3.5 elaborate the derivation of the DMVs and the corresponding coefficient matrices, which are defined in Eq. (5) to Eq. (8) by modeling each type of machining-induced variations.

3.2 Variations of Machine-Tool Axes. Machine-tools are typically composed of a kinematic chain of multiple translational and rotational axes that are designed to have only one degree of freedom (d.o.f.) of moving. However, due to geometric inaccuracy, misalignment and thermal effects, all these axes actually have deviations in three position d.o.f. and three rotational d.o.f. Intensive research has been conducted to estimate the positioning

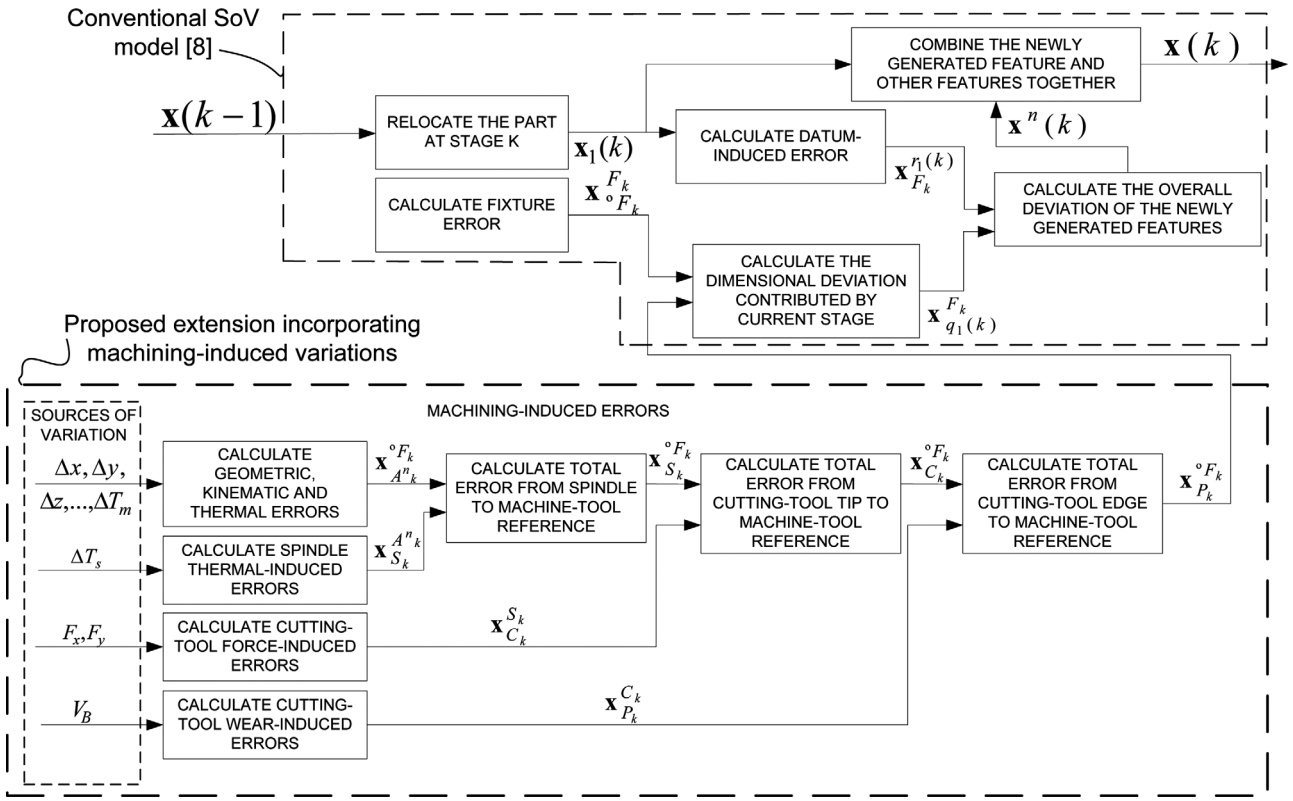

Fig. 6 Summary of the procedure to derive the extended state space model

errors of a cutting-tool in multi-axis machine-tools using rigid-body kinematics and HTMs [12,15,22]. With these methods, the position and orientation of each axis of a machine-tool, relative to each other or to the MCS, is modeled using a HTM. After determining the HTMs of all the movable links, they are multiplied successively from the last axis to the MCS, resulting in the actual position of the CS of the last axis w.r.t. the MCS. Considering an n-axis machine-tool, the final position of A^n_k w.r.t. $^{\circ}M_k$ can be defined as

$$\mathbf{H}^{\circ M_k}_{A^n_k} = \mathbf{H}^{\circ M_k}_{\circ A^n_k} \cdot \delta\mathbf{H}^{\circ M_k}_{A^n_k} = \mathbf{H}^{\circ M_k}_{\circ A^1_k} \cdot \delta\mathbf{H}^{\circ M_k}_{A^1_k} \cdot \prod_{i=2}^{n} \mathbf{H}^{\circ A^{i-1}_k}_{\circ A^i_k} \cdot \delta\mathbf{H}^{A^{i-1}_k}_{A^i_k} \quad (12)$$

where $\mathbf{H}^a_b$ is the HTM of CS b w.r.t. CS a, and $\delta\mathbf{H}^a_b$ is the HTM that defines the small position and orientation deviations of CS b w.r.t. a due to the deviation from nominal values of b and a. With the assumption of rigid-body kinematics and small-angle approximation, any differential transformation matrix $\delta\mathbf{H}^{A^{i-1}_k}_{A^i_k}$ can be generally defined as a product of three HTMs [12,15,22], i.e.,

$$\delta\mathbf{H}^{A^{i-1}_k}_{A^i_k} = \begin{pmatrix} 1 & -\varepsilon_{zi} & \varepsilon_{yi} & \delta_{xi} \\ \varepsilon_{zi} & 1 & -\varepsilon_{xi} & \delta_{yi} \\ -\varepsilon_{yi} & \varepsilon_{xi} & 1 & \delta_{zi} \\ 0 & 0 & 0 & 1 \end{pmatrix} \cdot \begin{pmatrix} 1 & -\varepsilon_z(i) & \varepsilon_y(i) & \delta_x(i) \\ \varepsilon_z(i) & 1 & -\varepsilon_x(i) & \delta_y(i) \\ -\varepsilon_y(i) & \varepsilon_x(i) & 1 & \delta_z(i) \\ 0 & 0 & 0 & 1 \end{pmatrix} \cdot \begin{pmatrix} 1 & -E^{\gamma i}_t & E^{\beta i}_t & E^{xi}_t \\ E^{\gamma i}_t & 1 & -E^{\alpha i}_t & E^{yi}_t \\ -E^{\beta i}_t & E^{\alpha i}_t & 1 & E^{zi}_t \\ 0 & 0 & 0 & 1 \end{pmatrix} \quad (13)$$

The first HTM describes the mounting errors of the ith axis w.r.t. the $(i-1)$th axis. The mounting errors are position and orientation errors due to assembly imperfections and they are independent of the carriage position. Mounting errors can be represented by two of three possible angular deviations ε_{xi} (rotation around the X-axis), ε_{yi} (rotation around the Y-axis) and ε_{zi} (rotation around the Z-axis), and three offsets (δ_{xi}, δ_{yi}, δ_{zi}). The second HTM represents the motional deviations, which include the terms $\delta_p(q)$ and the terms $\varepsilon_p(q)$. $\delta_p(q)$ refers to the positional deviation in the p-axis direction when the prismatic joint moves along the q-axis and is a function of the position of the q-axis. $\varepsilon_p(q)$ refers to the angular deviation around the p-axis when the q-axis moves and is also a function of the position of the q-axis. The third HTM describes the geometrical deviations due to thermal effects, whose components are defined as E^{pq}_t. E^{pq}_t includes scalar and position-dependent thermal components [12]. Mathematically, E^{pq}_t is generally defined by the equation

$$E^{pq}_t = f^{pq}_0(T_1, \ldots, T_m, t) + f^{pq}_1(T_1, \ldots, T_m, t) \cdot q + f^{pq}_2(T_1, \ldots, T_m, t) \cdot q^2 + \ldots. \quad (14)$$

The term $f^{pq}_0(T_1, \ldots, T_m, t)$ is a scalar thermal component that models the position deviation of the p-axis when the q-axis moves and it is a function of time, t, and the temperatures $T_1,\ldots,T_m$, measured at different locations of the machine-tool structure. The term $f^{pq}_1(T_1, \ldots, T_m, t) \cdot q + f^{pq}_2(T_1, \ldots, T_m, t) \cdot q^2 + \ldots$ is a position-dependent thermal component that models the position deviation on the p-axis when the q-axis moves.

Equation (13) shows that geometrical deviations caused by kinematic and thermal effects may have nonlinear relationships. In order to include these sources of variation into the SoV model, a linearization should be conducted based on three important assumptions. First, it is assumed that the geometric-thermal deviations are modeled when the machine-tool is warmed-up adequately and thus, the effect of time on the thermal deviations can be neglected. Second, it is assumed that the workpiece is repeatedly placed in the same region inside the allowable work space of the machine-tool table and thus, only small deviations at the placement of the workpiece are expected. Third, it is assumed that geometric, kinematic, and thermal deviations do not change

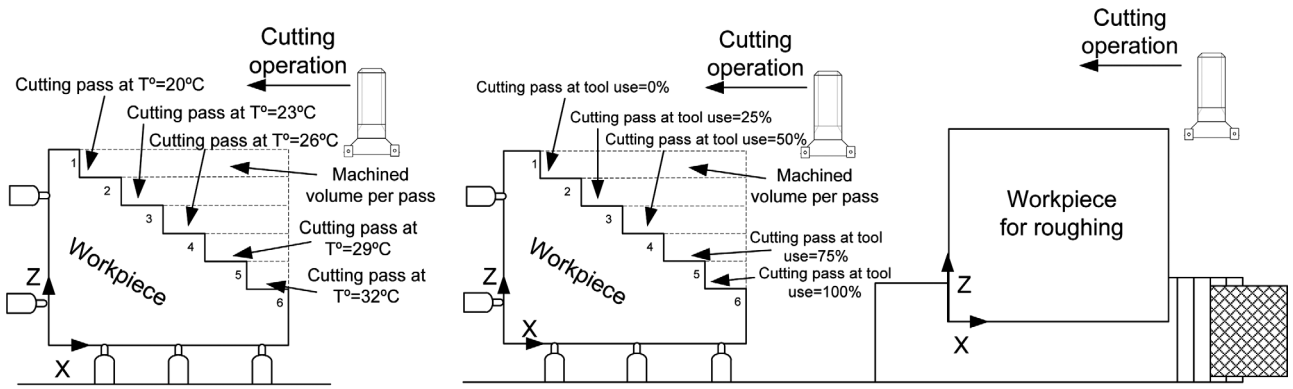

(a) Spindle thermal effects (b) Cutting-tool wear

Fig. 7 Experimentation to model machining-induced variations

drastically during the travels along any axis (the experimentation in Ref. [12] holds this assumption). As a result, the geometric-thermal deviations in a machine-tool axis can be linearized without significant loss of precision. Under these assumptions, the motional deviations $\delta_p(q)$ and $\varepsilon_p(q)$ are linearized as $\delta_p(q_0) + \frac{\delta(\delta_p(q))}{\delta q}|_{q=q_0} \cdot \Delta q$ and $\varepsilon_p(q_0) + \frac{\delta(\varepsilon_p(q))}{\delta q}|_{q=q_0} \cdot \Delta q$, respectively, where q_0 is the nominal placement of the workpiece on the q-axis, and Δq is the deviation of the workpiece placement on the machine-tool table from nominal values along the q-axis. On the other hand, the thermal-induced deviations E_t^{pq} from Eq. (14) can be linearized as

$$E_t^{pq} = C_0^{pq} + C_1^{pq} \cdot \Delta T_1 + \cdots + C_m^{pq} \cdot \Delta T_m + C_{m+1}^{pq} \cdot \Delta q \tag{15}$$

where $C_{(\cdot)}^{pq}$ are constants, ΔT_ρ is the deviation of the cth temperature point at the machine-tool structure from its nominal values $T_{\rho 0}$ where $\rho = 1,\ldots,m$.

As a conclusion, the resulting position and orientation deviations defined by the matrix $\delta \mathbf{H}_{A_k^n}^{\circ M_k}$, considering the linearization, can be obtained from Eq. (12). This matrix will be defined in the form of

$$\delta \mathbf{H}_{A_k^n}^{\circ M_k} = \begin{pmatrix} 1 & -\theta_{A_k^n z}^{\circ M_k} & \theta_{A_k^n y}^{\circ M_k} & d_{A_k^n z}^{\circ M_k} \\ \theta_{A_k^n z}^{\circ M_k} & 1 & -\theta_{A_k^n x}^{\circ M_k} & d_{A_k^n y}^{\circ M_k} \\ -\theta_{A_k^n y}^{\circ M_k} & \theta_{A_k^n x}^{\circ M_k} & 1 & d_{A_k^n z}^{\circ M_k} \\ 0 & 0 & 0 & 1 \end{pmatrix} \tag{16}$$

which can be further rewritten in a DMV as

$$\mathbf{x}_{A_k^n}^{\circ M_k} = \mathbf{B}_k^{m_1} \cdot [\Delta T_1^k, \ldots, \Delta T_m^k, (\Delta \mathbf{r}^k)^T]^T \tag{17}$$

In Eq. (17), $\Delta \mathbf{r}^k$ denotes the deviation of the workpiece placement on the machine-tool table along the nth axes. When a 5-axis machine-tool with A-axis and B-axis is modeled, $\Delta \mathbf{r}^k = [\Delta x^k, \Delta y^k, \Delta z^k, \Delta \alpha^k, \Delta \beta^k]$, where $\Delta\alpha$ and $\Delta\beta$ denote the deviation of the workpiece placement on A-axis and B-axis from linearized values, respectively. Please note that we discard the systematic deviations due to linealization such as the terms C_0^{pq}, $\delta_p(q_0)$, $\varepsilon(q_0)$, since they can be eliminated by an initial calibration.

For practical purposes, geometric and thermal parameters related to geometric-thermal-induced variations can be estimated from the experimental data. Research works [12,23–25] show in detail the derivation of these parameters.

3.3 Spindle Thermal-Induced Variations. The spindle-thermal variations are an important contributor to the total thermal variations during machining due to the large amounts of heat generated at high-speed revolutions [26]. Spindle thermal errors produce three positioning and two rotational drifts to the spindle CS [12]. These errors are represented as the deviation of the °SCS w.r.t. ACS^n and are proportional to the increase of the spindle temperature, ΔT_s, from nominal conditions. At station k, this deviation is defined by the DMV

$$\mathbf{x}_{S_k}^{A_k^n} = \left[f_1^k(\Delta T_s^k)\ \ f_2^k(\Delta T_s^k)\ \ f_3^k(\Delta T_s^k)\ \ f_4^k(\Delta T_s^k)\ \ f_5^k(\Delta T_s^k)\ \ f_6^k(\Delta T_s^k)\right]^T \approx \left[Cf_x^k\ \ Cf_y^k\ \ Cf_z^k\ \ Cf_\alpha^k\ \ Cf_\beta^k\ \ 0\right]^T \cdot \Delta T_s^k = \mathbf{B}_k^{m_2} \cdot \Delta T_s^k \tag{18}$$

where $f_i^k(\cdot)$ is a function that relates position and orientation errors of S_k to the deviation of the spindle temperature from nominal conditions. Cf_i^k are proportional coefficients linearizing the $f_i^k(\cdot)$ functions and the $f_6^k(\Delta T_s^k)$ is 0 since it is assumed that the cutting-tool rotations axis is Z. These coefficients can be obtained through the experimentation.

The experimentation consists of milling different workpiece surfaces at different spindle-thermal states, as shown in Fig. 7(*a*). To avoid fixture-induced variations, a workpiece with accurate datum surfaces should be mounted on a 3-2-1 fixture scheme during the entire procedure of the experiment. Several end milling operations are conducted with new cutting inserts at different spindle temperatures. The end milling operations are defined to manufacture the workpiece in the form of a "ladder" to make it possible to measure the surfaces generated at each operation. The spindle temperature is measured by a sensor of temperature. For each end milling operation, the temperature of the spindle is increased by rotating the spindle at a higher speed. After milling at different temperatures, the workpiece is measured in a Coordinate Measuring Machine (CMM) and the dimensional deviations of the milled surfaces can be linearly adjusted with respect to the spindle temperature.

3.4 Cutting Force-Induced Variations. The geometric variations of the machined workpieces due to cutting force-induced variations can be modeled by the cutting-tool deflection during the machining process. Various methods for cutting-tools with different complexity have been applied to model the deflection [16–18]. To represent this type of deflection and the corresponding variations with the SoV model, it is necessary to describe the position and orientation deviations of the cutting-tool due to the deflection. Assuming (i) the cutting depth of the finishing operations is insignificant compared with the length of the cutting-tool overhang, and (ii) the cutting force acts at the tool tip, the cutting-tool can be modeled as a unique cantilever beam defined by the equivalent tool diameter [18]. Then, the cutting-tool's displacement perpendicular to the cutting-tool axis is proportional to the cutting force, according to the equation [27]

$$\delta_r = \frac{F \cdot L^3}{3 \cdot E \cdot I} = \frac{64 \cdot F \cdot L^3}{3 \cdot \pi \cdot E \cdot D^4} \tag{19}$$

where E is the Young's Modulus for the material tool; L^3/D^4 is the tool slenderness parameter, where D is the equivalent tool diameter and L is the overhang length; and F is the cutting force perpendicular to the tool axis. Furthermore, the rotation of the tool tip along axis θ perpendicular to the cutting-tool axis is defined as [27]

$$\delta_\theta = \frac{F \cdot L^2}{2 \cdot E \cdot I} = \frac{64 \cdot F \cdot L^2}{2 \cdot \pi \cdot E \cdot D^4} \tag{20}$$

where F is the force exerted by the cutting-tool perpendicular to the plane defined by the axis θ and the cutting-tool axis. Thus, the true cutting-tool CS, CCS, is deviated from the nominal °CCS due to the cutting force-induced deflection. The deviation of CCS w.r.t. SCS at station k can be expressed by the DMV as

$$\mathbf{x}_{C_k}^{S_k} = \mathbf{B}_k^{m_3} \cdot [\Delta F_x^k \quad \Delta F_y^k]^T \tag{21}$$

where $\mathbf{B}_k^{m_3} = [C_1, 0; 0, C_1; 0, 0; 0, C_2; C_2, 0; 0, 0]$, and C_1 and C_2 are defined by the cutting-tool characteristics at station k by the expression $C_1 = \frac{64L^3}{3\pi ED^4}$ and $C_2 = \frac{3C_1}{2L}$. ΔF_x^k and ΔF_y^k are the variation of the cutting force in X and Y directions from nominal conditions, respectively.

The parameters required to model the force-induced variations can be obtained directly by the geometry of the cutting-tool. For example, the equivalent tool diameter, D, for end mills is considered 0.8 times the nominal cutting-tool diameter since the cutting flutes reduce the resistant section [18]. In order to obtain the Young's modulus, an experimentation is required since the manufacturers of cutting-tools do not usually provide this value. In [18], two experimental methods are proposed to obtain the value of Young's modulus for cutting-tools.

3.5 Cutting-Tool Wear-Induced Variations. Cutting-tool wear is another important factor affecting dimensional part quality. Different types of wear can be defined in cutting-tools, such as crater wear and flank wear, etc. Among them, the flank wear (V_B) is the most commonly measured tool wear in industry to keep parts within dimensional specifications [28]. However, the impact of V_B on dimensional part quality highly depends on the machining operation and the geometry of the cutting-tool. For example, for those cutting-tools with a clearance angle of 6 deg and a rake angle of 0 deg, the amount of displacement of the cutting edge due to wear on the flank was tested to be around one-tenth of the width of the wear mark [29].

According to the CSs defined previously, the V_B modifies the geometry of the tool tip and causes the deviation of TPCS from °TPCS. The wear of the cutting-tool tip will result in a loss of effective radial and axial cutting depth and, thus, generates dimensional deviations. In order to model the effect of V_B on part quality, the following assumptions are considered: (i) flank wear is homogeneous; (ii) there are no other factors, such as the generation of a built-up edge, on the cutting-tool edge; and (iii) the cutting-tool edge is a sharp edge. Under these assumptions, the deviation of the machined surface in its normal direction (Z direction of L_k^j) is formulated as follows:

$$\delta_z = \frac{\tan(\alpha)}{(1 - \tan(\gamma) \cdot \tan(\alpha))} \cdot V_B \tag{22}$$

where α and γ are the clearance angle and the rake angle of the cutting inserts. According to Eq. (22), dimensional deviations are proportional to the flank wear magnitude and, thus, can be described with a proportional coefficient for a specific cutting operation and cutting-tool geometry [30].

Assuming that cutting-tool flank wear remains constant during the same cutting operation of one workpiece (this assumption holds in case that the workpiece to be machined is in small-medium size), the cutting-tool wear-induced deviation is modeled as the DMV of P_k w.r.t. C_k, i.e.,

$$\mathbf{x}_{P_k}^{C_k} = \left[g_1^k(V_{B_{ij}}^k) \quad g_2^k(V_{B_{ij}}^k) \quad g_3^k(V_{B_{ij}}^k) \quad g_4^k(V_{B_{ij}}^k) \quad g_5^k(V_{B_{ij}}^k) \quad g_6^k(V_{B_{ij}}^k) \right]^T \approx \left[0 \quad 0 \quad Cf_{V_{B_{ij}}}^k \quad 0 \quad 0 \quad 0 \right]^T \cdot V_{B_{ij}}^k = \mathbf{B}_k^{m_4} \cdot V_{B_{ij}}^k \tag{23}$$

where $g_i^k(\cdot)$ is a function that relates position and orientation errors of P_k with the flank wear of the cutting-tool. In Eq. (23), $V_{B_{ij}}^k$ refers to the flank wear of the ith cutting edge of the jth cutting-tool at the kth machining station and $Cf_{V_{B_{ij}}}^k$ is a proportional coefficient that linearizes the $g_i^k(\cdot)$ function. The $Cf_{V_{B_{ij}}}^k$ coefficients can be obtained from experimentation. Note that cutting-tool wear can also generate tool deflections due to the increase of cutting forces. These force-induced effects are modeled in Sec. 3.4.

The experimentation to be conducted for modeling the variations induced by the cutting-tool wear consists of the milling operations on different workpiece surfaces at different cutting-tool wear rates, as it is shown in Fig. 7(*b*). To avoid fixture-induced variations, a workpiece with accurate datum surfaces should be mounted on a 3-2-1 fixture scheme during all the experiment. Similarly, to avoid thermal-induced variations, the spindle temperature should be kept constant during the machining operations, cooling or heating the spindle accordingly if the temperature varies from the nominal value. In addition to this workpiece, a second workpiece is placed at the machine-tool table in order to conduct continuous machining operations to wear the cutting-tool. The experimental procedure consists of a cutting pass on the first workpiece with new cutting-tool inserts, keeping the spindle temperature constant. Then, several cutting passes are performed on the second workpiece to wear the cutting-tool. After that, V_B is measured without removing the cutting insert from the cutting-tool and the procedure is then repeated until the cutting-tool is totally worn. Each cutting pass on the first workpiece is conducted to manufacture the workpiece in a "ladder" form in order to measure the surfaces generated by the cutting passes. When the tool is totally worn, the workpiece is removed and placed in a CMM using the same workpiece setup, and a linear regression between the cutting-tool wear and the dimensional deviations measured can be fitted. From this regression, the proportional coefficient $\{Cf_{V_{B_{ij}}}^k\}$ can be obtained.

4 Case Study

To validate the extended SoV model, we consider the case study on the machining of an Aluminum 6061 part shown in Fig. 8. The three-station machining process is illustrated in Fig. 9, with the datum features and the surfaces to be machined summarized in Table 1. The location of each fixture locator is given in Table 2. The nominal position and orientation of each workpiece

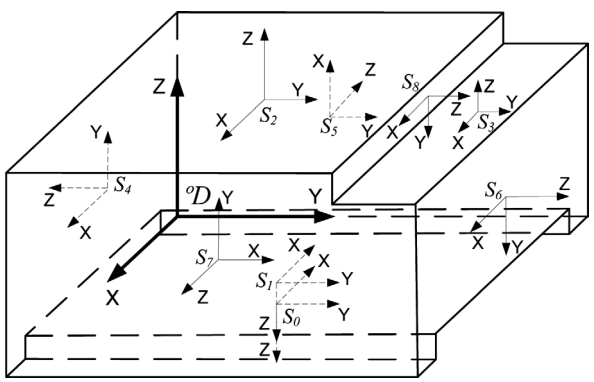

Fig. 8 Aluminum 6061 part investigated by the case study. Surface CSs from S_0 to S_8

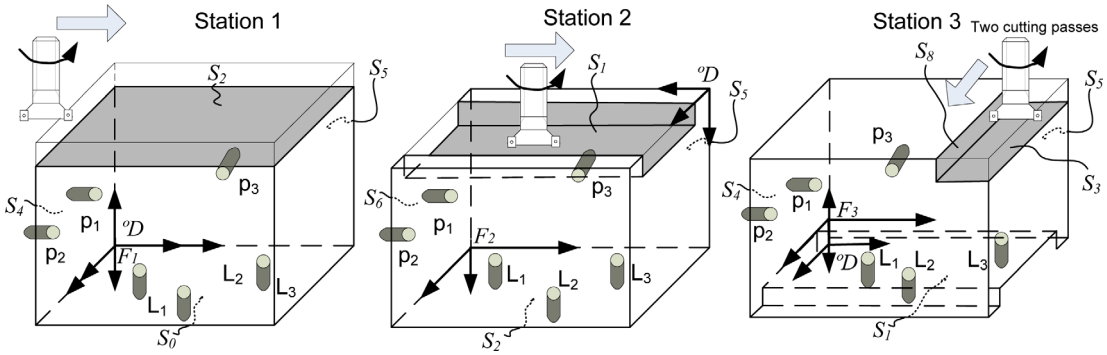

Fig. 9 A three-station machining process

Table 1 Process description of the case study

Station	Datum features	Features machined	Cutting-tool
1	$S_0 - S_4 - S_5$	S_2	ADHX 110305, PVD TiAlN $\phi = 24.856$ mm, $L = 111.322$ mm
2	$S_2 - S_6 - S_5$	S_1	ADHX 110305, PVD TiAlN $\phi = 24.856$ mm, $L = 111.322$ mm
3	$S_1 - S_4 - S_5$	S_3, S_8	ADHX 110305, PVD TiAlN $\phi = 24.856$ mm, $L = 111.322$ mm
4	$S_0 - S_4 - S_5$	CMM	

Note: ADHX: Indexable inserts (manufacturer code); PVD: Physical Vapor Deposition; ϕ: Tool diameter; L: Tool length.

Table 2 Nominal position and orientation of FCS w.r.t. °DCS and fixture layout

St.	$(\omega_{F_k}^{\circ D})^T$ (rad)	$(\mathbf{t}_{F_k}^{\circ D})^T$ (mm)	Locators (mm)
1	[−π/2,π,0]	[0,0,0]	$L_{1x} = 10, L_{1y} = 30, L_{2x} = 50, L_{2y} = 70, L_{3x} = 90, L_{3y} = 30$ $p_{1y} = 30, p_{1z} = -35, p_{2y} = 70, p_{2z} = -35, p_{3x} = 50, p_{3z} = -20$
2	[−π/2,0,0]	[0,95,45]	$L_{1x} = 10, L_{1y} = 30, L_{2x} = 50, L_{2y} = 70, L_{3x} = 90, L_{3y} = 30$ $p_{1y} = 30, p_{1z} = -35, p_{2y} = 70, p_{2z} = -35, p_{3x} = 50, p_{3z} = -20$
3	[−π/2,π,0]	[0,0,2.5]	$L_{1x} = 10, L_{1y} = 30, L_{2x} = 50, L_{2y} = 70, L_{3x} = 90, L_{3y} = 30$ $p_{1y} = 30, p_{1z} = -35, p_{2y} = 70, p_{2z} = -35, p_{3x} = 50, p_{3z} = -20$

Note: $\mathbf{t}_{F_k}^{\circ D}$ Nominal position of FCS w.r.t. °DCS; $\omega_{F_k}^{\circ D}$: Nominal orientation of FCS w.r.t. °DCS

Table 3 Product design information. Nominal position and orientation of each feature

Feature	$(\omega_{S_i}^{\circ D})^T$ (rad)	$(\mathbf{t}_{S_i}^{\circ D})^T$ (mm)
S_0	[0,π,0]	[47.5,47.5,0]
S_1	[0,π,0]	[47.5,47.5,2.5]
S_2	[0,0,0]	[47.5,42.5,45]
S_3	[0,0,0]	[47.5,90,40]
S_4	[π/2,−π/2, −π/2]	[47.5,0,22.5]
S_5	[0, −π/2,0]	[0,47.5,22.5]
S_6	[π/2,π/2, −π/2]	[47.5,95,20]
S_7	[0,π/2,π/2]	[95,47.5,22.5]
S_8	[π/2,π/2, −π/2]	[47.5,85,42.5]

Note: $\mathbf{t}_{S_i}^{\circ D}$:Nominal position; $\omega_{S_i}^{\circ D}$: Nominal orientation

surface are presented in Table 3. After station 3, the machined part is moved to the inspection station to measure the three KPCs defined by the manufacturing features S_2, S_3, and S_8. Note that features S_3 and S_8 are generated by the same cutting-tool, but with different cutting edges. S_3 is generated by the primary cutting edge, whereas feature S_8 is generated by the secondary cutting edge. To simplify the machining experimentation, the three machining stations presented in the case study are defined with the same machine-tool, cutting-tool, and fixture layout but with different datum features, as shown in Fig. 9. In order to compare both conventional and extended SoV models, five machining conditions were tested considering both fixture-induced and machining-induced variations.

In the first experiment, a workpiece was machined according to the process plan with minimum fixture and machining variations. For this purpose, the fixture locators were calibrated on the machine-tool table with a touch probe to ensure that the fixture assembly deviations are less than ± 0.015 mm. The machining operations were conducted with a spindle temperature close to 21 °C. The possible spindle temperature variations were compensated by a linear compensation algorithm provided by the machine-tool manufacturer. To control the impact of cutting-tool wear effects, a new cutting-tool was used in the experiment, whose dimensions were also calibrated with a mechanical touch probe on the machine-tool table. In addition, the workpiece clamping at each station was performed by a torque wrench to ensure a constant clamping force. With these settings, the MMP should generate high quality parts.

The second experiment only dealt with fixture-induced variations, keeping under control the machining-induced variations. The experiment was conducted in a similar way as the first experiment, except that some locator deviations were intentionally introduced, as shown in Table 4. These locators deviations were measured on the machine-tool table by a touch probe. For this experiment, the KPC deviations are mostly generated by the fixture-induced variations, and it can be adequately predicted by the conventional SoV model.

The third, the fourth, and the fifth experiments were conducted to evaluate the effects of machining-induced variations. In these experiments, the clamping procedure was kept the same as the second experiment but other locator deviations were introduced. In the third experiment, the temperature at the machine-tool spindle was increased to 25 °C (ΔT = 10 °C) without using any thermal compensation algorithm so a thermal deviation was present at all stations. The cutting-tool used was a new one in order to avoid cutting-tool wear effects. In the fourth experiment, the cutting operations at all stations were performed with a worn cutting-tool, without thermal variations. The cutting-tool flank wear was measured at both cutting-tool edges, with the resulting values of 0.9 mm and 0.5 mm for the primary and secondary cutting edges, respectively. Finally, in the fifth experiment, the spindle temperature was increased to 30 °C (ΔT = 15 °C) and a worn cutting-tool was used with a flank wear of 0.3 mm at both primary and secondary edges, keeping the same locator deviations as in the second experiment. In the third, the fourth, and the fifth experiments, the

Table 4 Experimental conditions

Exp	Error	Δl_1	Δl_2	Δl_3	Δp_1	Δp_2	Δp_3	ΔT_s	V_{B11}	V_{B21}
ID	type	(mm)	(mm)	(mm)	(mm)	(mm)	(mm)	(°C)	(mm)	(mm)
1	None	−0.008	0.000	0.012	−0.018	−0.004	0.000	0	0	0
2	LC	**−0.041**	0.000	**0.096**	−0.018	−0.004	0.000	0	0	0
3	LC and TH	**−0.024**	0.000	**−0.037**	−0.018	−0.004	0.000	**10**	0	0
4	LC and TW	**−0.024**	0.000	**−0.037**	−0.018	−0.004	−0.00	0	**0.9**	**0.5**
5	LC, TH and TW	**−0.041**	0.000	**0.096**	−0.018	−0.004	0.000	**15**	**0.3**	**0.3**

Note: LC: Locator deviation; TW: Cutting-tool wear; TH: Spindle thermal expansion. Note that all deviations apply to stations 1, 2 and 3.

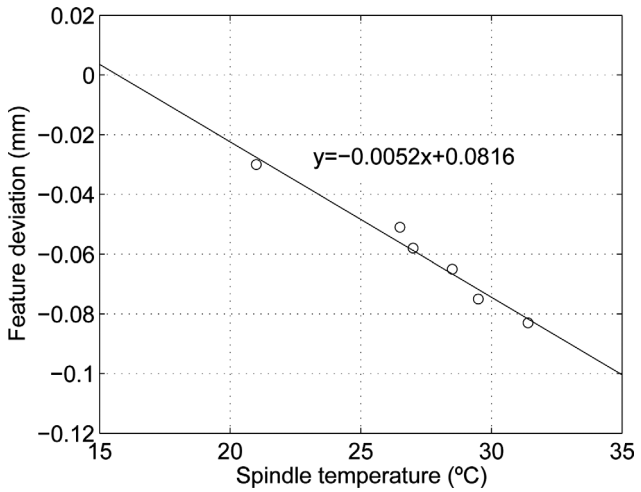

Fig. 10 Relationship between feature deviation and the spindle temperature

prediction errors of the conventional SoV model are expected to be higher than those in the second experiment due to the influence of the machining-induced variations. Furthermore, in these experiments, the extended SoV model is expected to be more accurate than the conventional model due to its ability to deal with the machining-induced variations.

4.1 Results and Discussion. In order to integrate the machining-induced variations, an experimentation for modeling purposes was conducted according to the steps mentioned in Sec. 3. For spindle-thermal variations, only the spindle thermal expansion in Z direction was studied. The spindle temperature was measured by a PT-100 sensor and the machine-tool was warmed up by keeping the spindle rotating at 10,000 r.p.m. After milling at different temperatures, the workpiece was measured in a CMM and the deviations between the machined features were linearly adjusted with the spindle temperature (Fig. 10). From the experimental results, the thermal coefficients were adjusted as: $Cf_x^k = Cf_y^k = Cf_\alpha^k = Cf_\beta^k = Cf_\gamma^k \approx 0$ and $Cf_z^k = -0.0052\,\text{mm}/^\circ\text{C}$ for $k = 1,2,3$. Note that the negative sign indicates that a thermal increase impacts on the deviation of the SCS along $-Z$ direction of the SCS and therefore, along the $-Z$ direction of the LCS^j.

On the other hand, in order to model the cutting-tool wear effects, several end milling operations were conducted with different cutting-tool flank wear values. The experimentation was conducted on a calibrated fixture device and keeping the spindle temperature at 25 °C. The end mill modeled was a cutter plate with inserts ADHX 110305, PVD TiAlN. The resulting linear relationships between flank wear values at primary and secondary cutting edges and the dimensional deviation of the machined features are shown in Fig. 11. From the experimental results, the cutting-tool wear coefficients were adjusted to: $Cf_{V_{B_{11}}}^1 = Cf_{V_{B_{11}}}^2 = Cf_{V_{B_{11}}}^3 = 0.125$ and $Cf_{V_{B_{21}}}^3 = 0.135$.

According to the experimental results, the quality of the machining operation is closely related to the cutting-tool wear, especially for features generated by the secondary cutting-tool edge (e.g., the machined feature S_8). The influence of the spindle thermal expansion is also important since, with a reasonable thermal spindle expansion of ±5 °C, a feature deviation around ±0.026 mm is expected. Other machining-induced variations, such as the geometric, kinematic, and thermal variations of machine-tool axes or cutting-tool deflections during machining, could also be considered. However, for this case study, one can expect that some of these sources of variation will be less important. For instance, if the workpieces are always placed in the same region of the machine-tool table, and the workpieces are small, one can expect

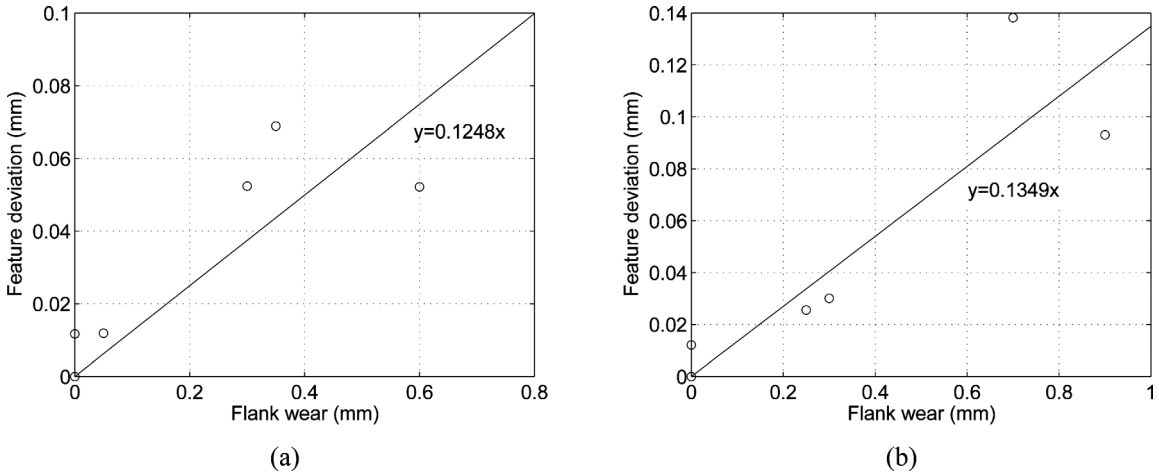

Fig. 11 Relationship between machined feature deviations and: (*a*) flank wear at the primary cutting-tool edge, and (*b*) flank wear at the secondary cutting-tool edge

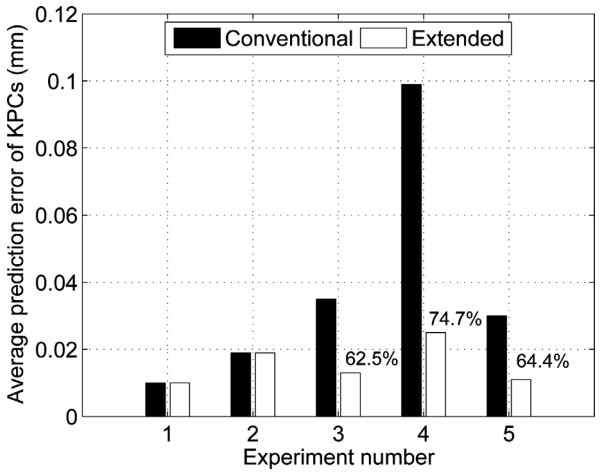

Fig. 12 Comparison of the average prediction errors in the five experimental conditions

that the geometric-kinematic variations during machining will be low. On the other hand, if the cutting-tools used are cutter plate tools, which are more robust than slender solid end mills, one can expect that cutting force-induced variations will be lower than those from slender solid end mills. In other words, the specific characteristics of the machining operation have to be considered in order to ensure that some of these machining-induced variations are negligible in comparison with others.

After modeling the relationships between machining-induced variations and part quality, the five experiments were conducted. After each cutting experiment, it was computed the average prediction error of the three KPCs according to the estimations from both conventional and extended SoV models. The average prediction errors of the five experimental conditions are shown in Fig. 12. Analyzing the results from the experiment 1, one can observe the difficulties to control all factors to ensure high quality. In spite of the control of locator deviations, spindle thermal expansion, cutting-tool wear, cutting-tool length and diameter calibration, and clamping deviations, the machined parts have still uncontrolled sources of variation which produce an average prediction error of 0.010 mm. Mainly, these factors could be dimensional deviations due to geometric-thermal effects on machine-tool axis, cutting-tool deflections or workpiece deformations due to cutting forces. For the second experiment, the machined part is deviated from its nominal values due to the locator deviations introduced at locators L_1 and L_3. The SoV model approximates the expected part quality fairly well with an average prediction error of 0.019 mm, validating the model for propagating errors in MMPs due to fixture-induced variations. The addition of machining-induced variations in the third, the fourth, and the fifth experiments reveal the limitation of the conventional SoV model predictions under these conditions. The extended SoV model is able to partially deal with these deviations and reduces the prediction error considerably. As shown in Fig. 12, the prediction improvement in the third, the fourth, and the fifth experimental conditions was 62.5%, 74.7%, and 64.4% respectively, which means an average prediction improvement of 67% with respect to the conventional SoV when machining-induced variations are applied.

5 Conclusion

In spite of the success of the SoV approach for variation propagation modeling in MMPs, the absence of machining-induced variations in the model may be an important factor to limit the use of this methodology for accurate variation prediction. In order to improve the conventional SoV model, it is desirable to additionally represent the machining-induced variations in a comprehensive model. In this paper, a generic framework for incorporating the machining-induced variations into the conventional SoV model is proposed. This generic framework requires experiments for the estimation of empirical models of machining-induced variations. Consequently, the approach is in particular interesting for applications in mass production where the costs for the initial calculation of the models can be compensated by the reduction of measurements of the variations during and after the multistation machining process.

The proposed model is compared with the conventional SoV model when different machining-induced variations are added in a MMP. The machining-induced variations modeled and added into the experimentation were related to spindle thermal expansion and cutting-tool wear. Different machining-induced variations were combined in the experimentation and the resulting prediction errors from the extended SoV model were notably lower (67% on average less) than those from the conventional SoV model, verifying the potential use of the extended SoV model proposed.

A fundamental assumption underlying the proposed methodology is the small magnitude of the variations. The extended model will keep under reasonable accuracy when the main sources of variation present small deviations from their nominal values. The study on the impacts of variation magnitudes on model accuracy will be further investigated in future research. Following the proposed framework, additional types of machining-induced variations can be included into the extended model through the chain of CSs that composes the machine-tool. Furthermore, the proposed comprehensive state space model can be applied: (i) to improve the accurateness of the conventional SoV model by considering new sources of variations, and (ii) to solve some problems in MMPs that have not been investigated yet. In the first application, conventional SoV applications, such as design evaluation of MMPs, tolerance analysis, and sensor placement, can be significantly improved by considering more variation sources. In the second application, the inclusion of these new variation sources can aid the investigation of new problems, such as machining fault diagnosis, complete manufacturing tolerance allocation, and new maintenance strategies integrating both fixture maintenance and cutting-tool replacement policies.

Acknowledgment

This work has been partially supported by Fundació Caixa-Castelló Bancaixa (Research Promotion 2007 and 2009). The authors greatly acknowledge the investigation support by the NSF Engineering Research Center for Reconfigurable Manufacturing System at University of Michigan. The authors would also like to thank the editors and reviewers for their insightful comments and suggestions, which have significantly improved the paper quality and readability.

Nomenclature

CS = coordinate system
DCS = design CS, denoted by D
RCS = reference CS, denoted by R
FCS = fixture CS, denoted by F
ACS^i = CS of axis i, denoted by A^i
LCS^j = CS of feature j, denoted by L^j
SCS = spindle CS, denoted by S
CCS = cutting-tool CS, denoted by C
TPCS = cutting-tool tip CS, denoted by P
MCS = machine-tool CS, denoted by M
$\mathbf{d}_2^1$ = position deviations of CS 1 with respect to (w.r.t.) CS 2, $\left[\Delta x_2^1 \quad \Delta y_2^1 \quad \Delta z_2^1\right]^T$
$\mathbf{s}_2^1$ = orientation deviations of CS 1 w.r.t. CS 2, $\left[\Delta\alpha_2^1 \quad \Delta\beta_2^1 \quad \Delta\gamma_2^1\right]^T$
$\mathbf{x}_2^1$ = deviation motion vector of CS 1 w.r.t. CS 2, $\left[(\mathbf{d}_2^1)^T \quad (\mathbf{s}_2^1)^T\right]^T$
$\mathbf{H}_2^1$ = homogeneous transformation matrix between CS 1 and CS 2

Appendix

Proof of Lemma 1. Noting $\mathbf{H}_1^R = \mathbf{H}_{\circ 1}^R \cdot \delta\mathbf{H}_1^R$, we have $\mathbf{H}_R^1 = (\mathbf{H}_1^R)^{-1} = (\delta\mathbf{H}_1^R)^{-1} \cdot \mathbf{H}_R^{\circ 1}$. Then, considering $\mathbf{H}_2^1 = \mathbf{H}_R^1 \cdot \mathbf{H}_2^R$ we have

$$\mathbf{H}_2^1 = (\mathbf{H}_1^R)^{-1} \cdot \mathbf{H}_2^R = (\delta\mathbf{H}_1^R)^{-1} \cdot \mathbf{H}_R^{\circ 1} \cdot \mathbf{H}_2^R \tag{A1}$$

As $\mathbf{H}_2^R = \mathbf{H}_{\circ 2}^R \cdot \delta\mathbf{H}_2^R$, Eq. (A1) is rewritten as

$$\mathbf{H}_2^1 = (\delta\mathbf{H}_1^R)^{-1} \cdot \mathbf{H}_R^{\circ 1} \cdot \mathbf{H}_{\circ 2}^R \cdot \delta\mathbf{H}_2^R \tag{A2}$$

Noting $\delta\mathbf{H}_2^R$ as

$$\delta\mathbf{H}_2^R = \mathbf{I}_{4\times 4} + \Delta_2^R \tag{A3}$$

where Δ_2^R is the differential transformation matrix defined as

$$\Delta_2^R = \begin{pmatrix} \widehat{\theta}_2^R & \mathbf{d}_2^R \\ \mathbf{0} & 0 \end{pmatrix} \tag{A4}$$

where $\widehat{\theta}_2^R$ is the skew matrix of θ_2^R and it is defined as

$$\widehat{\theta}_2^R = \begin{pmatrix} 0 & -\theta_{2z}^R & \theta_{2y}^R \\ \theta_{2z}^R & 0 & -\theta_{2x}^R \\ -\theta_{2y}^R & \theta_{2x}^R & 0 \end{pmatrix} \tag{A5}$$

and considering the small motion assumption (then, $\Delta_R^1 = -\Delta_1^R$, as shown in Ref. [8]), Eq. (A2) can be rewritten as

$$\mathbf{H}_2^1 = (\mathbf{I}_{4\times 4} - \Delta_1^R) \cdot \mathbf{H}_{\circ 2}^{\circ 1} \cdot (\mathbf{I}_{4\times 4} + \Delta_2^R) \tag{A6}$$

As $\mathbf{H}_2^1 = \mathbf{H}_{\circ 2}^{\circ 1} \cdot \delta\mathbf{H}_2^1$, from Eq. (A6) we can derive $\delta\mathbf{H}_2^1$ as

$$\delta\mathbf{H}_2^1 = (\mathbf{H}_{\circ 2}^{\circ 1})^{-1} \cdot \left(\mathbf{H}_{\circ 2}^{\circ 1} - \Delta_1^R \cdot \mathbf{H}_{\circ 2}^{\circ 1} + \mathbf{H}_{\circ 2}^{\circ 1} \cdot \Delta_2^R - \Delta_1^R \cdot \mathbf{H}_{\circ 2}^{\circ 1} \cdot \Delta_2^R\right) \tag{A7}$$

Neglecting the second-order small values and re-ordering

$$\Delta_2^R = (\mathbf{H}_{\circ 2}^{\circ 1})^{-1} \cdot \Delta_1^R \cdot \mathbf{H}_{\circ 2}^{\circ 1} + \delta\mathbf{H}_2^1 - \mathbf{I}_{4\times 4} \tag{A8}$$

Considering the following properties of skew-symmetric matrices

$$\mathbf{a} \times \mathbf{b} = \widehat{\mathbf{a}} \cdot \mathbf{b} \tag{A9}$$

$$\mathbf{a} \times \mathbf{b} = (\widehat{\mathbf{b}})^T \cdot \mathbf{a} \tag{A10}$$

$$\mathbf{A}^T \cdot \widehat{\mathbf{a}} \cdot \mathbf{A} = \mathbf{A}^T \cdot \mathbf{a} \tag{A11}$$

where $\widehat{\mathbf{a}}$ is the skew-symmetric matrix of vector $\mathbf{a}$, and $\times$ is the cross product operator, then Eq. (A8) can be rewritten in a vector form resulting in Eq. (1).

References

[1] Shi, J., 2007, *Stream of Variation Modeling and Analysis for Multistage*, CRC Press/Taylor&Francis Group, Boca Raton, FL.

[2] Montgomery, D. C., 1996, *Introduction to Statistical Quality Control*, John Wiley & Sons, Hoboken, NJ.

[3] Jin, J., and Shi, J., 1999, "State Space Modeling of Sheet Metal Assembly for Dimensional Control," ASME J. Manuf. Sci. Eng., **121**, pp. 756–762.

[4] Huang, W., Lin, J., and Kong, Z., 2007, "Stream-of-Variation (SOVA) Modeling II: A Generic 3D Variation Model for Rigid Body Assembly in Multi-Station Assembly Processes," ASME J. Manuf. Sci. Eng., **129**, pp. 832–842.

[5] Liu, J., Jin, J., and Shi, J., 2010, "State Space Modeling for 3-D Variation Propagation in Rigid-Body Multistage Assembly Processes," IEEE Trans. Autom. Sci. Eng., **7**(2), pp. 274–290.

[6] Huang, Q., Shi, J., and Yuan, J., 2003, "Part Dimensional Model Error and its Propagation Modeling in Multi-Operational Machining Processes," ASME J. Manuf. Sci. Eng., **125**, pp. 255–262.

[7] Djurdjanovic, D., and Ni, J., 2003, "Dimensional Errors of Fixtures, Locating and Measurement Datum Features in the Stream of Variation Modeling in Machining," ASME J. Manuf. Sci. Eng., **125**(4), pp. 716–730.

[8] Zhou, S., Huang, Q., and Shi, J., 2003, "State Space Modeling of Dimensional Variation Propagation in Multistage Machining Process Using Differential Motion Vectors," IEEE Trans. Rob. Autom., **19**(2), pp. 296–309.

[9] Abellan-Nebot, J. V., Liu, J., and Romero, F., 2009, "Limitations of the Current State Space Modeling Approach in Multistage Machining Processes Due to Operation Variations," AIP Conf. Proc., **1181**(1), pp. 231–243.

[10] Ramesh, R., Mannan, M. A., and Poo, A. N., 2000, "Error Compensation in Machine Tools—A Review Part I: Geometric, Cutting-Force Induced and Fixture-Dependent Errors," Int. J. Mach. Tools Manuf., **40**(9), pp. 1235–1256.

[11] Ramesh, R., Mannan, M. A., and Poo, A. N., 2000, "Error Compensation in Machine Tools—A Review Part II: Thermal Errors," Int. J. Mach. Tools Manuf., **40**(9), pp. 1257–1284.

[12] Chen, J. S., Yuan, J., and Ni, J., 1996, "Thermal Error Modelling for Real-Time Error Compensation," Int. J. Adv . Manuf. Technol., **12**, pp. 266–275.

[13] Baradie, M. A. E., 1996, "The Effect of Varying the Workpiece Diameter on the Cutting Tool Clearance Angle in Tool-Life Testing," Wear, **195**(1-2), pp. 201–205.

[14] Suh, S.-H., Lee, E.-S., and Jung, S.-Y., 1998, "Error Modelling and Measurement for the Rotary Table of Five-Axis Machine Tools," Int. J. Adv . Manuf. Technol., **14**, pp. 656–663.

[15] Lei, W. T., and Hsu, Y. Y., 2002, "Accuracy Test of Five-Axis CNC Machine Tool With 3D Probe-Ball. Part I: Design and Modeling," Int. J. Mach. Tools Manuf., **42**(10), pp. 1153–1162.

[16] Kim, G. M., Kim, B. H., and Chu, C. N., 2003, "Estimation of Cutter Deflection and Form Error in Ball-End Milling Processes," Int. J. Mach. Tools Manuf., **43**, pp. 917–924.

[17] Dow, T. A., Miller, E. L., and Garrard, K., 2004, "Tool Force and Deflection Compensation for Small Milling Tools," Precis. Eng., **28**, pp. 31–45.

[18] López de Lacalle, L. N., Lamikiz, A., Sanchez, J. A., and Salgado, M. A., 2004, "Effects of Tool Deflection in the High-Speed Milling of Inclined Surfaces," Int. J. Adv . Manuf. Technol., **24**, pp. 621–631.

[19] Bi, X., Liu, Y., and Liu, Y., 2009, "Analysis and Control of Dimensional Precision in Turning Process," *Proceedings of Control and Decision Conference*, pp. 3456–3459.

[20] Joshi, P., 2003, *Jigs and Fixtures Design Manual*, McGraw-Hill, New York.

[21] Paul, R., 1981, *Robot Manipulator: Mathematics, Programming, and Control*, MIT Press, Cambridge, MA.

[22] Choi, J. P., Lee, S. J., and Kwon, H. D., 2003, "Roundness Error Prediction With a Volumetric Error Model Including Spindle Error Motions of a Machine Tool," Int. J. Adv . Manuf. Technol., **21**, pp. 923–928.

[23] Chen, G., Yuan, J., and Ni, J., 2001, "A Displacement Measurement Approach for Machine Geometric Error Assessment," Int. J. Mach. Tools Manuf., **41**(1), pp. 149–161.

[24] Yang, S. H., Kim, K. H., Park, Y. K., and Lee, S. G., 2004, "Error Analysis and Compensation for the Volumetric Errors of a Vertical Machining Centre Using a Hemispherical Helix Ball Bar Test," Int. J. Adv . Manuf. Technol., **23**, pp. 495–500.

[25] Tseng, P. C., 1997, "A Real-Time Thermal Inaccuracy Compensation Method on a Machining Centre," Int. J. Adv . Manuf. Technol., **13**(3), pp. 182–190.

[26] Haitao, Z., Jianguo, Y., and Jinhua, S., 2007, "Simulation of Thermal Behavior of a CNC Machine Tool Spindle," Int. J. Mach. Tools Manuf., **47**(6), pp. 1003–1010.

[27] Gere, J. M., and Goodno, B. J., 2008, *Mechanics of Materials*, 7th ed., Nelson Engineering, Toronto.

[28] ISO 8688-1:1989, *Tool-Life Testing in Milling—Part 1: Face Milling*.

[29] Warnecke, G., and Kluge, R., 1998, "Control of Tolerances in Turning by Predictive Control With Neural Networks," J. Intell. Manuf., **9**(4), pp. 281–287.

[30] Sheikh, A. K., Raouf, A., Sekerdey, U. A., and Younas, M., 1999, "Optimal Tool Replacement and Resetting Strategies in Automated Manufacturing Systems," Int. J. Prod . Res., **37**(4), pp. 917–937.